

Melt Infiltration Processing of Foams Using Glass-Forming Alloys

C. San Marchi, A. Brothers, and D. C. Dunand

Department of Materials Science & Engineering, Northwestern University, Evanston, IL 60208

ABSTRACT

Processing of foams from bulk metallic glass (BMG) alloys, using melt infiltration techniques, is reported for the first time. Foaming methods based on infiltration of two types of pattern materials are described: investment of a continuous refractory yielding very low relative density structures (5% dense relative to the BMG), and investment of a discontinuous refractory pellet bed yielding higher relative density (50-60% dense relative to the BMG). Both methods are capable of producing foam structures; however high surface area and diminished thermal conductivity, especially in lower density structures, make vitrification of the alloy difficult.

INTRODUCTION

The development of metallic alloys with strong glass-forming ability has enabled processing of bulk amorphous components with exceptionally high strength (around 2 GPa for Zr-based alloys in compression) and excellent resistance to corrosion and wear [1,2]. However when loaded beyond the elastic limit, glass-forming alloys are prone to catastrophic shear localization and failure without significant ductility (often <1%), making them unreliable for critical structural applications. One method of avoiding this problem has been to introduce additional phases such as ceramics, ductile metals, or native crystalline phases into the amorphous alloy [3-7]. Although a marked improvement in fracture strain can be achieved in such composites, the choice of reinforcement is limited by issues of reaction/dissolution and heterogeneously nucleated crystallization at the matrix/reinforcement interface, resulting in a density that is often significantly higher than that of the monolithic glass. As for metallic foams, BMG foams offer a reduction in density along with predicted increases in several material indices such as specific stiffness and strength, mechanical energy absorption, and acoustic damping [8]; furthermore, there is the possibility of shear band confinement and consequent improvements to macroscopic ductility in BMG foams.

Although crystalline metals and alloys have been successfully foamed by these techniques, no report has yet been made of an amorphous metal foam. In this report, we describe recent developments in processing of foams from BMG alloys, according to two methods based on melt infiltration of pattern materials, which show promise for the production of strong, lightweight amorphous metal foams.

EXPERIMENTAL PROCEDURES

Two types of pattern materials were used for melt infiltration experiments: continuous refractory preforms and discontinuous graphite preforms. Refractory slurries were used to create molds based on commercially available open-cell polyurethane foams of 5% relative density (Foamcraft, Inc., Skokie, IL). Polyurethane foams were cut into cylinders with 12.7 mm diameter and 25.4 mm height. These cylinders were wrapped with an impermeable film, placed on an absorbent surface, and invested with small amounts of a refractory slurry. Invested cylinders

were centrifuged to improve settling of the slurry, and dried directionally on a hot plate. After drying was complete, more slurry was added, and the process was repeated until the entire cylinder was contained within the dried ceramic mold. Molds were then slowly heated in air to 500°C to burn out the polyurethane, leaving a ceramic mold containing a network of open channels identical to the struts of the original foam.

In the second process, graphite powder and water were blended with small amounts (~1 wt. %) of NaF salt as a binder, and then tumbled. Tumbling for one hour agglomerated the powder into pellets with sizes ranging from the submillimeter range up to several millimeters or more. Collected pellets were dried and then coated prior to packing with an aerosol graphite lubricant, whose small particle size helped protect pellet surfaces from infiltration by the melt. Agglomerates were strong enough to be sieved and packed into beds for use as a pattern material.

Buttons of the glass-forming alloy $Zr_{57}Nb_5Cu_{15.4}Ni_{12.6}Al_{10}$ (Vit106) were produced by arc melting high-purity elemental metals several times under a Ti-gettered argon atmosphere. Vit106 buttons were then cut to be placed on a perforated high-density graphite disk which rested on the pattern materials and served to prevent premature contact between melt and pattern. Patterns and disks were placed inside quartz crucibles (inner diameter: 10-14 mm, wall thickness: 1 mm) coated with graphite to improve wetting and prevent reduction of the quartz by the melt. Crucibles were suspended from wires within a quartz tube by means of a magnet attached to the outside of the tube, which was situated between two radiant line heaters and attached to a manifold which allowed the vessel atmosphere to be controlled.

After vacuum-baking the pattern materials, crucibles, and disks at the processing temperature (917 °C, or 75-100 °C above the liquidus, which varies depending on exact composition) to remove volatiles, BMG was added on top of the disk, and the vessel was evacuated and heated again to the same temperature at an average heating rate of 6 °C/s. A period of 7 minutes was allowed for melting and homogenization to occur, during which the Vit106 melt pooled against the crucible wall, isolating the evacuated pattern from the rest of the apparatus. An applied positive pressure of 50 kPa high-purity Ar was then used to drive the melt into the open volume of the pattern material. After holding the system under pressure for 4 minutes to ensure complete infiltration, the suspending magnet was removed and the samples allowed to drop into a bath of strongly agitated brine (8.5% NaCl aqueous) solution chilled to 0 °C. It was determined that pure Vit106 melts equilibrated at the processing temperature in quartz crucibles having 1 mm wall thicknesses and inner diameters up to 12 mm could be vitrified (within the limits of x-ray detection) using this quenching process.

Foam structure was characterized by scanning electron microscopy (SEM) with a Hitachi model S-3500N microscope, and crystallinity was assessed by x-ray diffraction (XRD) using $Cu-K\alpha$ radiation in a Rigaku Geigerflex diffractometer. Uniaxial compressive tests were performed using a Sintech 20/G screw-driven load frame with a nominal strain rate of $9.4 \cdot 10^{-4} s^{-1}$.

RESULTS AND DISCUSSION

Continuous Refractory Patterns (Investment Casting Technique)

Several slurries were considered as investments for the replication process, the most successful being graphite, zirconia, yttria, and combinations thereof. Graphite powder investments were investigated first, since their relatively high thermal conductivity suggested the

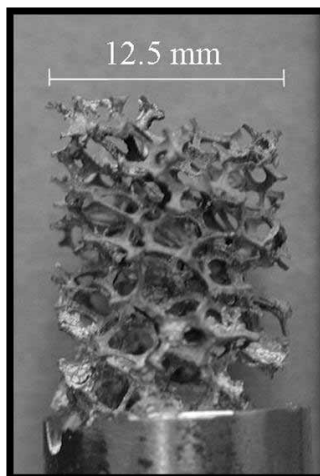


Figure 1: Macroscopic architecture of a Vit106 foam, processed using a polyurethane foam cylinder coated with graphite and invested with yttria slurry.

best prospects of vitrification of the alloy. It was found that graphite investments suffered mild drying shrinkage but lacked mechanical integrity and could not be handled without breaking once the polymer had been burned out. Blending graphite with zirconia slurry in a 3:1 volume ratio diminished drying shrinkage and improved integrity, but the investment was difficult to remove and foam materials were very brittle, likely due to formation of ZrC (identified by XRD, not shown) on the large surface area of exposed BMG. Formation of ZrC in Vit106 after infiltration of WC, TiC, and SiC powders has been observed previously, where it was found not to cause heterogeneous nucleation of the alloy [3,4]; consequently the unusual brittleness of these samples likely results from brittleness of the ZrC layer itself rather than from any unusual amount of crystallinity.

Zirconia-based slurries showed no clear evidence of reaction with the melt and were very strong; however shrinkage during drying led to distorted foam structures and difficulty in removing the pattern after infiltration. Removal could only be accomplished by severe mechanical picking, which caused damage to the small features of the foam. Also, it has been suggested by Altounian et al. [9] that ZrO_2 may contribute to crystallization of some Zr-based alloys due to its crystallographic similarity with the native crystalline phase Zr_2Ni .

The best results were achieved with yttria investments, which were found to be stable at high temperatures, suffer little shrinkage and distortion during drying, have good mechanical integrity, and be relatively easy to remove after infiltration. Yttria preforms could be handled gently without risk of damage and showed no outward signs of cracking during the drying process. Removal of the investment was accomplished by a combination of mechanical picking, strong jets of water, and ultrasonic agitation in organic solvents. Yttria has been used extensively in investment casting of reactive alloys, particularly Ti-based alloys, because of its very high stability. Moreover, Zhang *et al.* [10] have shown that addition of Y to several Zr-Al-Ni-Cu and Zr-Ti-Cu-Ni-Be alloys enhances glass-forming ability, perhaps by scavenging oxygen and preventing formation of the more harmful ZrO_2 nuclei.

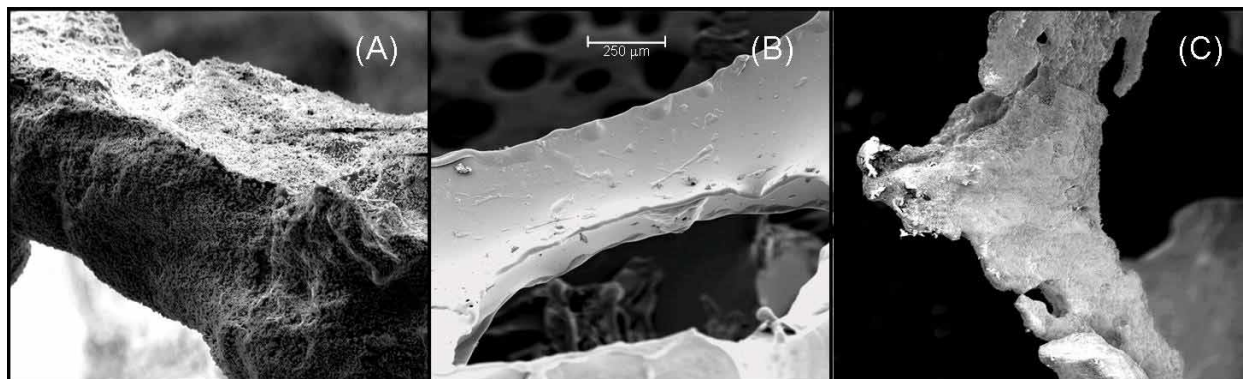


Figure 2: SEM micrographs showing: (A) An intact strut made of Vit106 using an yttria preform; (B) a similar strut in the original polyurethane foam, coated with 25 nm of Au to prevent specimen charging; (C) A flawed strut from the same Vit106 foam as the strut in part (A), resulting from infiltration of defects in the yttria preform. Scale bars on all three micrographs are the same.

An example of the foam architecture achievable with yttria investments is presented in Figure 1, which confirms that replication of the polyurethane foam structure is possible. In Figures 2a and 2c, individual struts in a similar Vit106 foam also processed using yttria investment are examined using SEM. The strut shown in Figure 2a has a morphology very similar to that of the original polyurethane foam (Fig. 2b); the strut in Figure 2c, by contrast, appears to have resulted from infiltration of a flaw in the pattern. Flaws of this nature could be caused by incomplete settling of the slurry, cracking induced by drying shrinkage, or damage inflicted during handling; further work is needed to clarify the cause of such flaws and methods for their prevention.

Figure 3a shows x-ray diffraction (XRD) results taken from a section of the BMG foam in Fig. 2 that was powdered in a mortar and pestle. The pattern clearly shows a number of crystalline peaks which are not associated with yttria or any other oxides native to the system, and which closely resemble peaks seen in a sample of pure Vit106 vacuum-annealed at 500°C for 3 days (not shown). This crystallinity is at least partially responsible for the poor mechanical properties of the foam replicas, which are extremely brittle (although less so than samples processed using graphite) and crush at nearly zero stress (0.1 to 0.2 MPa) with no appreciable strain. Also at fault may be structural flaws of the sort shown in Fig. 2c. At present it is not clear to which degree each factor limits macroscopic mechanical behavior.

The high degree of crystallinity seen in the replicated foam, pending analysis of oxygen content in the BMG [11], suggests that cooling in the melt was slow, which was partially the result of the poor thermal conductivity of the yttria powder pattern. From this perspective an attractive alternative to oxide investments are salt investments, which have higher thermal conductivity, do not contribute to oxygen contamination in the melt, may be sintered for strength, and are more easily removed by dissolution after infiltration. At present, however, no salt has been identified which is chemically compatible with Vit106 at the processing temperature. Sodium fluoride, for example, was found to decompose at the processing temperatures under vacuum; reaction with gaseous products led to formation of a skin on the BMG surface and prevented the pooling that is required for pressure infiltration. Similar results were found with K_2SO_4 and with the mixed oxide lithium orthosilicate (Li_4SiO_4), which was

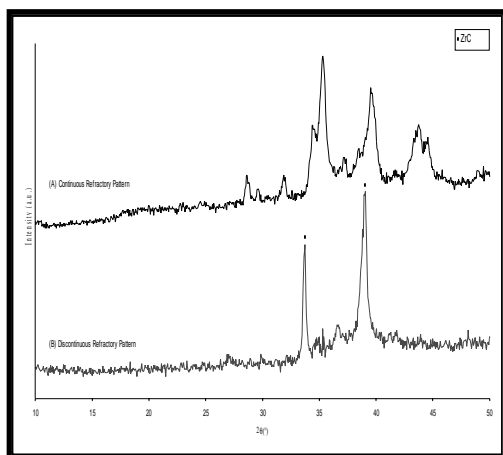


Figure 3: XRD patterns from (A) Vit106 foam processed by the continuous refractory pattern method using pure yttria; (B) Vit106 foam processed by the discontinuous refractory pattern method using pellets made of graphite, NaF salt, and water.

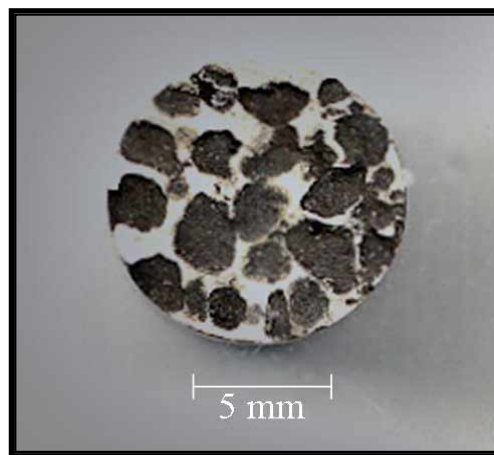


Figure 4: Cross-sectional image of a bed of pellets made of graphite, NaF salt, and water, then infiltrated with molten Vit106. Sample density is 3.91 g/cm^3 (relative density 57.4%).

investigated because it has high stability and melting point, yet partially dissolves in boiling water.

Discontinuous Refractory Patterns (Pellet Infiltration Technique)

Graphite pellets of the type described above, and having sizes in the range 1–3 mm, were found to have a bulk density of 1.1 g/cm^3 and a tap density of 0.67 g/cm^3 (i.e., a packing efficiency of ca. 60%). If these graphite pellets are not removed, the relative density achievable after infiltration is 50%. This relative density reflects the ideal case where infiltration produces foam whose pellets occupy precisely the same volume fraction as in the uninfiltrated state, and represents a lower bound on the relative density achievable in wetting systems such as graphite-BMG after real infiltrations.

Several pellet patterns were infiltrated with Vit106 as described above, giving foam specimens with diameters ranging from 10 mm to 14 mm and relative densities from 50–60%. Figure 4 shows a cross-section of one foam with 12 mm diameter, showing the size and distribution of the pellets. The density of this foam was measured to be 3.91 g/cc (relative density 57.4%), ca. 15% greater than the lower bound given above. This higher density reflects the fact that the smallest pellets became partially or fully infiltrated during processing, and that some pellets were crushed during handling and hence did not contribute porosity to the foam. In addition, it is noted that contact points between pellets were infiltrated, preventing removal of the pellets after infiltration. Although the low density of the pellets minimizes their impact on overall density, the possibility of dissolving patterns which maintain connectivity suggests again the use of salts as pattern materials.

The sample in Fig. 4 was loaded under uniaxial compression, leading to fracture after a linear 0.8% strain at a peak stress of 22.8 MPa, with no observable plastic deformation. The Young's modulus of the foam was 3.1 GPa. Elastic strain, compressive fracture strength, and Young's modulus of the bulk amorphous alloy are, respectively, 2%, 1800 MPa, and 84.7 GPa [5]. The poor mechanical response of the foam may be attributed to its crystallinity and to defects in the structure, the latter having an exaggerated effect due to the high ratio of pellet/pore

size to sample diameter [8]. Figure 3b shows XRD results from one of the fractured pieces of the sample, with the graphite mechanically removed to reveal fracture surfaces and pores as much as possible. Evident in the figure are a small amorphous background and two prominent peaks resulting from ZrC formed at the pellet/melt interface. Smaller reflections, indicating a limited degree of alloy crystallinity, are also present, although they too are obscured by the ZrC signal, which is strong due to the fact that the surfaces probed by the x-rays consisted largely of these interfaces (i.e., largely of hollowed out pellet pores). As described above, both the ZrC and the native crystallinity may have contributed to the poor mechanical response of the foam, but it is not yet clear what factor dominates.

CONCLUSIONS

Foam structures with very low (~5%) and moderate (50-60%) relative density have been successfully processed by melt infiltration of preforms using the glass-forming alloy Vit106. Despite achieving correct macroscopic foam architectures, foam strengths are poor due to lack of complete vitrification resulting from contamination due to high surface areas and reduction in effective thermal conductivity. Small flaws on the foam surfaces may also act as notches, contributing to early fracture. Further work is in progress to refine the present processing routes, and to employ pattern materials with improved conductivity and solubility, such as salts, leachable oxides, or blends of salts and oxides. In addition, work continues in alternate processing paths including gas entrapment in the melt, infiltration of hollow spheres, and powder metallurgical methods.

ACKNOWLEDGEMENTS

The authors gratefully acknowledge the ongoing support of the Defense Advanced Research Projects Agency's Structural Amorphous Metals (DARPA-SAM) Project and of the Caltech Center for Structural Amorphous Metals.

REFERENCES

- [1] Johnson, W.L. *Mat. Sci. Forum* **225-227** 35-50 (1996)
- [2] Wang, W.H., Wang, R.J., Fan, G.J. and J. Eckert. *Mater. Trans.* **42**(4) 587-591 (2001)
- [3] Choi-Yim, H. and W.L. Johnson. *App. Phys. Lett.* **71** 3808-3810 (1997)
- [4] Choi-Yim, H., Busch, R., Köster, U. and W.L. Johnson. *Acta Mater.* **47**(8) 2455-2462 (1999)
- [5] Conner, R.D., Choi-Yim, H. and W.L. Johnson. *J. Mater. Res.* **14**(8) 3292-3297 (1999)
- [6] Kuhn, U., Eckert, J., Mattern, N. and L. Schultz. *App. Phys. Lett.* **80**(14) 2478-2480 (2002)
- [7] Fan, C., Ott, R.T., and T.C. Hufnagel. *App. Phys. Lett.* **81**(6) 1020-1022 (2002)
- [8] Ashby, M.F., Evans, A., Fleck, N.A., Gibson, L.J., Hutchinson, J.W., and H.N.G. Wadley. *Metal Foams: A Design Guide*. Boston: Butterworth-Heinemann (2000)
- [9] Altounian, Z., Batalla, E. and J.O. Strom-Olsen. *J. App. Phys.* **61** 149-155 (1986)
- [10] Zhang, Y., Pan, M.X., Zhao, D.Q., Wang, R.J., and W.H. Wang. *Mater. Trans. JIM* **41**(11) 1410-1414 (2000)
- [11] Lin, X.H., Johnson, W.L., and W.K. Rhim. *Mater. Trans. JIM* **38**(5) 473-477 (1997)